Highlights of Spanish Astrophysics VIII, Proceedings of the XI Scientific Meeting of the Spanish Astronomical Society held on September 8–12, 2014, in Teruel, Spain. A. J. Cenarro, F. Figueras, C. Hernández-Monteagudo, J. Trujillo Bueno, and L. Valdivielso (eds.)

Nebular emission lines in high redshift galaxies

Esther Mármol-Queraltó[1], Ross McLure[1], and Fergus Cullen[1]

[1] SUPA, Institute for Astronomy, University of Edinburgh, Royal Observatory, Edinburgh EH9 3HJ, UK

Abstract

Recent works have shown that the specific star formation –defined as the ratio between the star formation rate (SFR) and the stellar mass– seems to evolve far less rapidly than expected in most theoretical models. Also, it has been claimed that the equivalent width (EW) of Hα evolves rapidly up to redshift $z \sim 8$. Both results rely on fitting their spectral energy distributions (SEDs) where rest-frame optical nebular emission lines (e.g., Hα) may contaminate the broad-band fluxes and bias the results inferred. In this work, we combine the best-available broad-band photometry in CANDELS with new near-infrared spectroscopy taken from the 3D-HST survey for a sample of star-forming galaxies at intermediate redshifts ($z \sim 1.3$) to test a method to infer reliable measurements of the Hα EW from the flux excess between observations and the best-fit model to their SEDs. Following this method, we revisit the photometric data available for galaxies up to $z \sim 5$ to trace the evolution of the equivalent width of Hα. In contrast with previous works, we find a mild evolution of Hα, much slower than the expected from the extrapolation of observations at lower redshifts.

1 Introduction

The evolution of the physical properties of galaxies such as the stellar mass and the star formation rate (SFR) have been (and are) extensively analysed using photometric data in a wide range of redshifts. However, these results rely on fitting their spectral energy distributions (SEDs) where rest-frame optical nebular emission lines (e.g., Hα) may contaminate the broad-band fluxes and bias the results inferred. Recent works have shown that the specific SFR seems to evolve far less rapidly than expected in most theoretical models [18, 8]. In addition, it has been claimed that the equivalent width (EW) of Hα evolves rapidly with redshifts, what would have an important impact in the SFR and stellar mass derived from the SED fitting.

In addition, the Hα EW should be a reasonable proxy for the specific SFR since it is defined as the ratio of the Hα total flux (a good star-formation indicator) to the flux density

of the underlying stellar continuum (the Hα continuum sits on the rest-frame r band, and therefore, is an indicator for the stellar mass). Thus, the rapid evolution pointed for EW(Hα) is difficult to understand now that it is reasonably well agreed that the evolution of the sSFR at $z > 2$ is either flat or slowly rising.

In this work, we infer the equivalent width of Hα using photometric data to explore its evolution up to $z \sim 5$ and compare it with the evolution of the specific SFR.

2 The data

In this work we combine two data-sets: the photometric data provided by the Cosmic Assembly Near-IR Deep Extragalactic Legacy Survey (CANDELS)[9, 12] and a spectroscopic sample selected from the 3D-HST spectroscopic survey [2, 15]. We restricted our work to the Great Observatories Origins Deep Survey southern field (GOODS-S) and the Ultra Deep Survey (UDS), both with accurate photometry in the K band available. The photometric data were taken from the existing CANDELS catalogues for GOODS-S [10] and UDS [7] fields, which cover from optical to mid-infrared bands.

2.1 Star formation rates and stellar masses: SED fitting

We fit a set of templates to the galaxy SEDs using the publicly available code `LePhare` [1, 11]. Our set of templates was built using the Bruzual & Charlot 2003 models [3] with solar ($Z_\odot$) and subsolar ($0.2\,Z_\odot$) metallitity, a Chabrier initial mass function (IMF) and a range of star-formation histories (SFHs) with exponentially decaying SFRs, the so-called τ-models with τ= 0.05, 0.1, 0.2, 0.3, 1, 2, 3, 5,10, 15, and 30 Gyr. We allow fits with two attenuation curves: the attenuation law for local starburst galaxies [4], and the extinction law for the Small Magellanic Cloud (SMC) [13], with $E(B-V)$ values ranging from 0 to 1.0 in steps of 0.01. Finally, the age of the model is allowed to vary between 50 Myr and the age of the Universe at the spectroscopic redshift of the galaxy.

2.2 Selection criteria

We focus our study in star-forming galaxies for which significant emission lines from their star-forming regions is expected. For this reason, we first matched our initial sample to the Chandra 4MS X-ray catalog in GOODS-S [19] to remove AGN from the initial sample.

It is now well established that there is a tight correlation between the SFR and the stellar mass for star-forming galaxies, called the main sequence of star-forming galaxies, with only $\sim 0.20 - 0.35$ dex of observed scatter. We follow the latest relation for the evolution of the main sequence with cosmic time derived by [16] to select our sample of star-forming galaxies. A final cut in stellar mass of $\log M > 9.0$ were applied to obtain complete galaxy samples at the different redshift ranges.

Finally, we select those galaxies for which we obtain accurate photometric redshifts ($\Delta z/(1+z) < 0.15$) and $\chi^2 < 25$ in their SED fitting. In addition, from the 3D-HST data

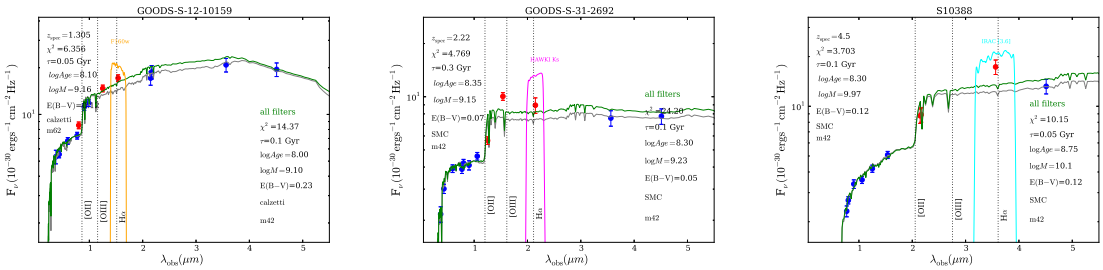

Figure 1: Examples of SEDs of spectroscopically confirmed galaxies at $z \sim 1.3, 2.2$, and 4.5. In each panel, the observed fluxes are plotted with circles, red colour for those filters where nebular emission lines are expected to be found at the given redshift. The response curves for those filters are also overplotted in each case. The best-fit model to the whole photometry is plotted in green, while the best-fit model to the photometry excluding the contaminated filters is plotted in grey. The insets quote the galaxy properties derived from the best-fit model in each case. It is clear a flux excess in the filter where the Hα emission line should be located in each case.

we selected galaxies in the GOODS-S fields in two redshift ranges: i) galaxies at $1.14 < z < 1.45$, for galaxies with prominent [OIII]λ4958,5007 and Hα+[NII] are observable within the grism wavelength range; and ii) galaxies at $2.00 < z < 2.30$, where [OII]λ3727, Hβ and [OIII]λ4958,5007 emission lines are included within the grism wavelength range. We also include 46 galaxies at $3.8 < z < 5.0$ in GOODS-S [14, 18] with data in our photometric catalogue. At this redshift range, Hα and [N II] will be found in IRAC-CH1 band, with no contamination of other lines in adjacent photometric bands. This will allow us to estimate their Hα EW.

3 Flux excess due to the nebular emission lines

Figure 1 shows three examples of the SED fitting of galaxies at $z \sim 1.3, 2.2,$ and 4.5 to the photometry excluding the the possible contaminated filters by emission lines. The flux excess observed for those bands where emission lines are expected according to their redshifts will be used to compute the line fluxes and equivalent widths. For comparison, it is also plotted the best-fit model when all the filters. In that case, the observed flux excess is significantly lower, pointing out to a much lower inferred EW.

4 Evolution of the equivalent width of Hα

We use the flux excess the observed and the synthetic photometry over the best-fit model in our samples of star-forming galaxies to infer the equivalent width of Hα at different redshifts. Our data-set allows us the study the evolution of Hα+[N II] at $z \sim 1.3, 2.2, 4.5$ from the flux excess in F160W, HAWKI-Ks and IRAC-CH1 bands, respectively. The results are presented

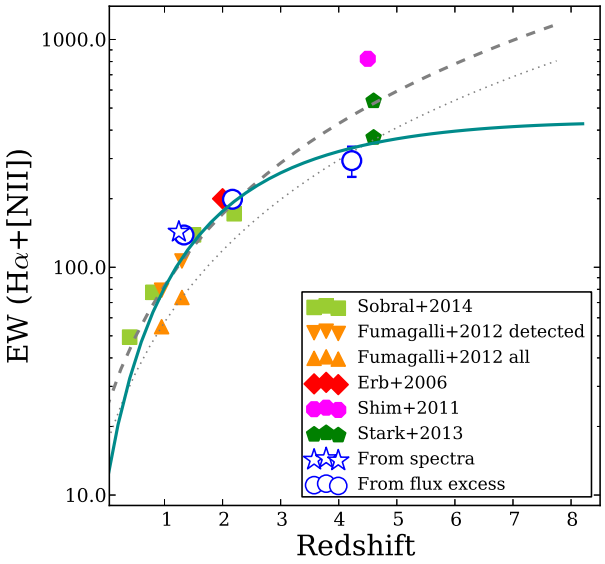

Figure 2: The evolution of the EW(Hα+[N II]) with redshift. The equivalent width have been computed from the flux excess of the observed photometry over the best-fit SED model. Open blue stars represent the samples in this study, while filled symbols show previous works in the literature, as indicated in the inset. The evolution of EW(Hα+[N II]) derived by [6] for galaxies with $M \sim 10^{10-10.5}\,\mathrm{M}_{\odot}$ up to $z \sim 2$ for galaxies with detected nebular emission and their whole sample is plotted with black dashed and dotted lines, respectively.

in Fig. 2, where the values for the EW(Hα+[N II]) inferred from the flux excess are presented with blue open circles, together with previous works in the literature. The evolution inferred by [6] for galaxies up to $z \leq 2$ with $M \sim 10^{10-10.5}\,\mathrm{M}_{\odot}$ is also plotted. The average of the stellar masses in the different samples analized in this work is $\sim 5 \times 10^{9}\,\mathrm{M}_{\odot}$. We find a good overall agreement of our EWs with previous works in the literature for galaxies at $z \leq 2$, both spectroscopic measurements (red diamond and orange triangles, respectively)[5, 6] and narrow band photometry (green squares) [17].

However, it is clear that for galaxies at higher redshift, the evolution of EW(Hα+[N II]) is lower than the expected from the extrapolation of the expression by [6] for their sample of galaxies with detected Hα+[N II], and similar to their estimation for their global sample which includes non detected sources. This is in contrast with the previous works by [14] and [18], who inferred EW(Hα+[N II]) 3 and 2 times higher than our results, respectively, and closer to the estimation by [6] for detected sources.

5 Conclusions

In this work, we combine the best-available broad-band photometry in CANDELS with new near-infrared spectroscopy taken from the 3D-HST survey for a sample of star-forming galax-

ies at intermediate redshifts ($z \sim 1.3$) to robustly test a method to infer reliable measurements of Hα from the flux excess between observations and the SED fitting. Following this method, we revisit the photometric data available for galaxies up to $z \sim 5$ to trace the evolution of the equivalent width of Hα. In contrast with previous works, we find a mild evolution of the Hα EW, much slower than the expected from the extrapolation of observations at lower redshifts [6, 17]. This evolution is compatible with the observed evolution of the specific SFR.

Acknowledgments

EMQ and RJM acknowledge the support of the European Research Council via the award of a Consolidator Grant (P.I.McLure), while FC acknowledges the support of the Science and Technology Facilities Council (STFC) via the award of an STFC Studentship. This work is based on observations taken by the CANDELS Multi-Cycle Treasury Program and the 3D-HST Treasury Program (GO 12177 and 12328) with the NASA/ESA HST, which is operated by the Association of Universities for Research in Astronomy, Inc., under NASA contract NAS5-26555.

References

[1] Arnouts S., Cristiani S., Moscardini L., et al. 1999, MNRAS, 310, 540

[2] Brammer, G. B., van Dokkum, P. G., Franx, M., et al. 2012, ApJS, 200, 13

[3] Bruzual, G., & Charlot, S. 2003, MNRAS, 344, 1000

[4] Calzetti, D., Armus, L., Bohlin, R. C., et al. 2000, ApJ, 533, 682

[5] Erb, D. K., Steidel, C. C., Shapley, A. E., et al. 2006, ApJ, 647, 128

[6] Fumagalli, M., Patel, S. G., Franx, M., et al. 2012, ApJL, 757, L22

[7] Galametz, A., Grazian, A., Fontana, A., et al. 2013, ApJS, 206, 10

[8] González, V., Bouwens, R., Illingworth, G., et. al. 2014, ApJ, 781, 34

[9] Grogin, N. A., Kocevski, D. D., Faber, S. M., et al. 2011, ApJS, 197, 35

[10] Guo, Y., Ferguson, H. C., Giavalisco, M., et al. 2013, ApJS, 207, 24

[11] Ilbert, O., Arnouts, S., McCracken, H. J., et al. 2006, A&A, 457, 841

[12] Koekemoer, A. M., Faber, S. M., Ferguson, H. C., et al. 2011, ApJS, 197, 36

[13] Prevot, M. L., Lequeux, J., & Prevot, L. 1984, A&A, 132, 389

[14] Shim, H., Chary, R. R., Dickinson, M., et al. 2011, ApJ, 738, 69

[15] Skelton, R. E., Whitaker, K. E., Momcheva, I. G., et al. 2014, ApJS, 214, 24

[16] Speagle, J. S., Steinhardt, C. L., Capak, P. L., & Silverman, J. D. 2014, ApJS, 214, 15

[17] Sobral, D., Best, P. N., Smail, I., et al. 2014, MNRAS, 437, 3516

[18] Stark, D. P., Schenker, M. A., Ellis, R., et al. 2013, ApJ, 763, 129

[19] Xue, Y. Q., Luo, B., Brandt, W. N., et al. 2011, ApJS, 195, 10